

## Influences of SiC Concentration on Sn/SiC Nanocomposite Electrodeposition

Hongtao Chu<sup>1,2,3</sup>, Jinqiu Zhang<sup>1,2</sup>, Maozhong An<sup>1,2\*</sup>

<sup>1</sup>State Key Laboratory of Advanced Welding and Joining, <sup>2</sup>School of Chemical Engineering and Technology, Harbin Institute of Technology, Harbin 150001, China

<sup>3</sup> College of Chemistry and Chemical Engineering, Qiqihar University, Qiqihar 161006, China

\*E-mail: [mzan@hit.edu.cn](mailto:mzan@hit.edu.cn)

*Received:* 3 December 2012 / *Accepted:* 18 January 2012 / *Published:* 1 February 2013

---

This paper studied the electrodeposition of Sn-SiC nanocomposite electrodeposits. The influences of SiC nanoparticle concentration in the plating bath on the surface morphology, composition, and properties were investigated by using X-ray diffraction, scanning electron microscope, transmission electron microscope, corrosion test, and Tafel test. The results revealed that SiC nanoparticle concentration has great influence on the composition of a surface. Within a certain range and with increasing SiC concentration, the crystal growth orientation changes and the coating grain becomes finer. The corrosion resistance of the coating improves with the increase of SiC content.

---

**Keywords:** surface morphology; composition; nano-SiC; composite electrodeposit

### 1. INTRODUCTION

Sn-Pb alloy coating is widely used in applications such as electronics and semiconductors because of its weldability and effectiveness in suppressing the growth of Sn whiskers. However, its application is also restricted because of the negative effects of lead on the environment. To obtain an alternative to Sn-Pb alloy coating, lead-free coating equipped with binary alloy coating such as Sn-Bi, Sn-Ag, Sn-Cu, and Sn-Zn as well as Sn-Ag-Cu[1] ternary coating was developed. However, this lead-free coating is not widely used because of its electrodeposition and substandard performance.

Composite electrodeposition is a new technology for improving coating performance and involves adding solid micron or nanoscale particles into the electroplate liquid. Electrodeposition deposits both solid particles and matrix metals in the matrix[2]. Larger micron particles are more prone

to gravity settling because particle size has a big impact on electrodeposition. Nanoscale particles have become a popular research topic in the electrodeposition field because it significantly reduces gravity settling effects. Nanoparticles that can be added include  $\text{Al}_2\text{O}_3$ , SiC, and  $\text{SiO}_2$ [3-7]. Nanoparticle composite coating is characterized by wear resistance, antifriction, thermostability, and corrosion resistance. In a study of prepared Ni-P-SiC nanocomposite coating, Nowa et al[8]. investigated the influences of nano-SiC content on the performance of the coating, which resulted in improved wear resistance and corrosion resistance along with increased SiC content in the coating. Zanella et al[9,10]. also reached similar conclusions from a study on Ni/SiC nanocomposite coating.

At present, the existed lead-free weldable coating is tin alloy coating. Compared with pure tin plating, it has been improved in corrosion resistance and suppression of Sn whiskers growth, but the preparing technology is complex and the cost is expensive. Nano composite electrodeposition is a new technology for improving the performance of traditional metal coating, and it has been applied in nickel base metal coating. Although only a few studies focus on the preparation and performance of composite coating of lead-free weldable Sn-nanoparticles, it is an innovation to introduce SiC nanoparticles into pure tin coating to improve the performance of weldable tin coating. This coating is widely used because it has a low melting point, good weldability, and corrosion resistance. With the introduction of SiC nanoparticles,  $\text{La}_2\text{O}_3$ , and WC particles into Au and Ag coatings, the formed composite coating became wear resistant, and electrical contact improved. Therefore, the addition of nanoparticles will greatly improve the performance of Sn composite coating.

By adding SiC nanoparticles into liquid Sn methyl sulfonate bath system and obtaining Sn-SiC nanoparticle composite coating through electrodeposition, this research observed the influence of SiC concentration on the composition, feature, structure, and corrosion resistance of the coating, which is significant to develop new types of weldable coating and improve performance of coating.

## 2. EXPERIMENT

### 2.1 SiC stability experiment

The aqueous solution was prepared by using cetyltrimethylammonium bromide, sodium dodecyl benzene sulfonate, and arabic gum as dispersing agents within the concentration range of 0.15 to  $0.45 \text{ g}\cdot\text{L}^{-1}$ . The stability of SiC was investigated by testing the absorbance change rate of nanoparticles in dispersing aqueous solution agents of different types and concentrations. The ratio of absorbance change rate and initial absorbance  $((A_i - A_0)/A_0)$  was observed in this experiment. (TEM) (HITACHI, H-7650) was used to observe the dispersibility of SiC.

### 2.2 Electroplating experiment

SiC nanoparticles were added into a liquid Sn methanesulfonic acid system with alkali liquor which is composed of  $30 \text{ g}\cdot\text{L}^{-1}\text{Na}_2\text{CO}_3 - 30 \text{ g}\cdot\text{L}^{-1}\text{NaHCO}_3$  and copper sheet matrix dipped in 30%

sulfuric acid solution as cathode and pure latten as anode, and successively went through mechanical stirring, continuous current, rack plating, and electrodeposition. The experiment was conducted under the following conditions:  $\text{Sn}(\text{CH}_3\text{SO}_3)_2$ :  $48.31 \text{ g}\cdot\text{L}^{-1}$ ;  $\text{CH}_3\text{SO}_3\text{H}$  (70%):  $80 \text{ g}\cdot\text{L}^{-1}$ ; hydroquinone:  $2 \text{ g}\cdot\text{L}^{-1}$ ; SiC nanoparticles (40 nm): 0 to  $10 \text{ g}\cdot\text{L}^{-1}$ ; dispersing agent:  $0.15 \text{ g}\cdot\text{L}^{-1}$  to  $0.45 \text{ g}\cdot\text{L}^{-1}$ ; stirring rate: 200 rpm; brightening agent:  $1 \text{ ml}\cdot\text{L}^{-1}$ ; electric current density:  $3 \text{ A}\cdot\text{dm}^{-2}$ ; anode:latten ( $4\times 4 \text{ cm}$ , purity  $>99.99\%$ ); cathode: copper foil ( $3\times 3 \text{ cm}$ , purity  $>99.99\%$ ); temperature:  $25 \text{ }^\circ\text{C}$ .

### 2.3 Coating representation

The corrosion resistance of the coating was investigated through the corrosion weight loss experiment of coating in  $\text{pH}=3.5$  acid solution and Tafel curve in 3.5% NaCl solution. The SiC content in composite coating was analyzed by using energy dispersive spectroscopy (EDS) (Horiba, EX-250). Microscopic appearance on the composite coating surface was observed by using scanning electron microscope (SEM) (Hitachi, S-4300). The composite structure of the coating surface was tested by using X-ray diffraction (XRD) (Bruker-AXS, D8 ADVANCE).

## 3.RESULTS AND DISCUSSION

### 3.1 SiC stability study

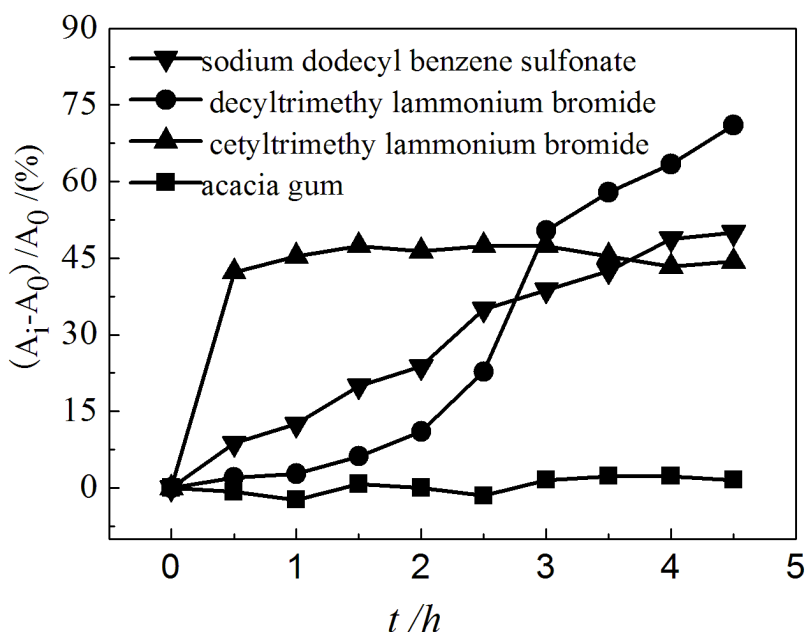


**Figure 1.** Influence of the dispersing agent on SiC stability.

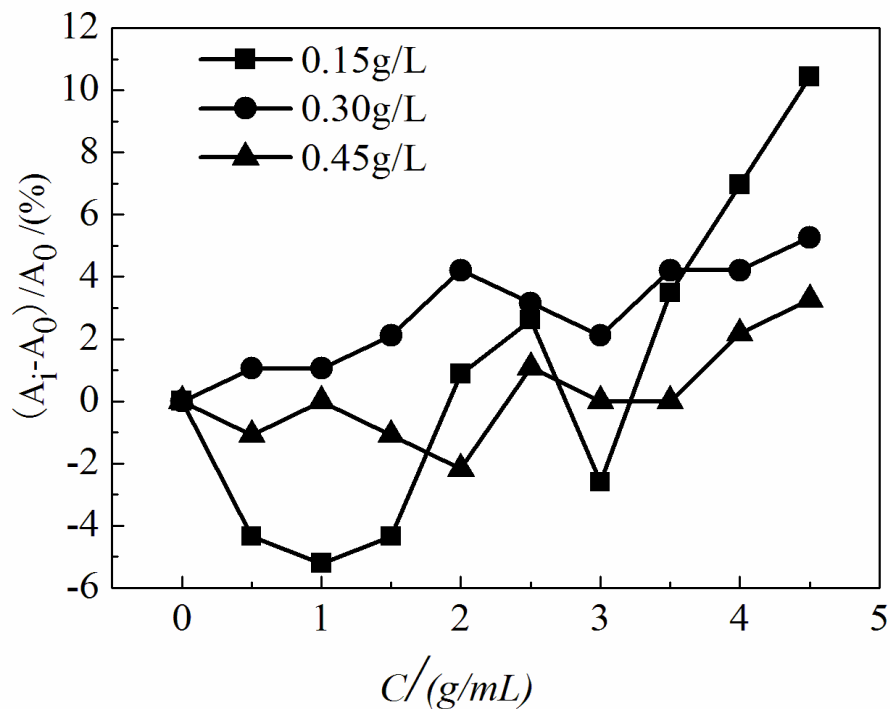
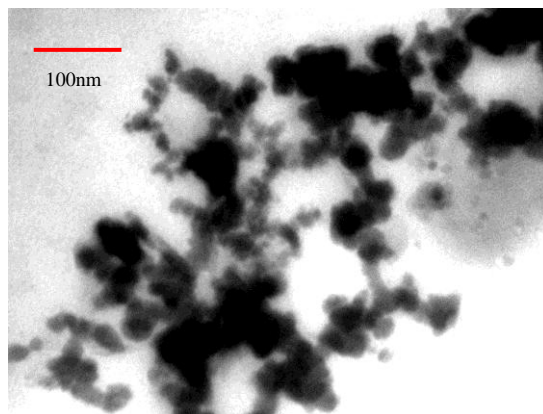


**Figure 2.** Influence of arabic gum concentration on SiC stability.

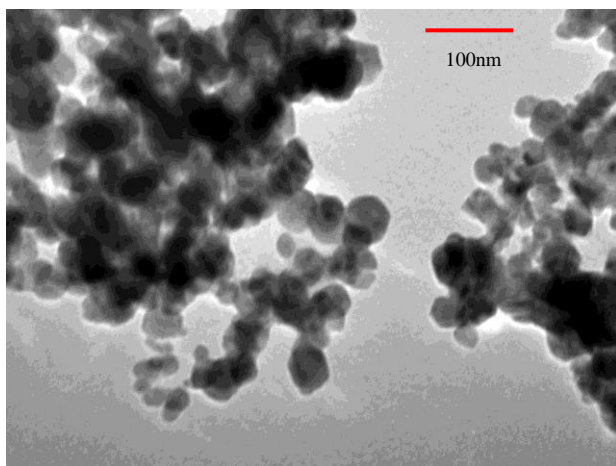
The nanoparticles subsided because of agglomeration during composite electrodeposition; small particle size and high surface energy affected electrodeposition. To improve the stability of particles[11], the frequently used method is to add a surfactant to the coating solution, which serves as a dispersing agent.

SiC was added to the surfactant solution to prepare a turbid liquid which successively went through 5 h of mechanical stirring and 1 h of sonic oscillation. Then, a spectrophotometer was used to test the time and the change of absorbance of the turbid liquid at 310 nm. The influences of dispersing agent types on SiC stability are shown in Figure 1.

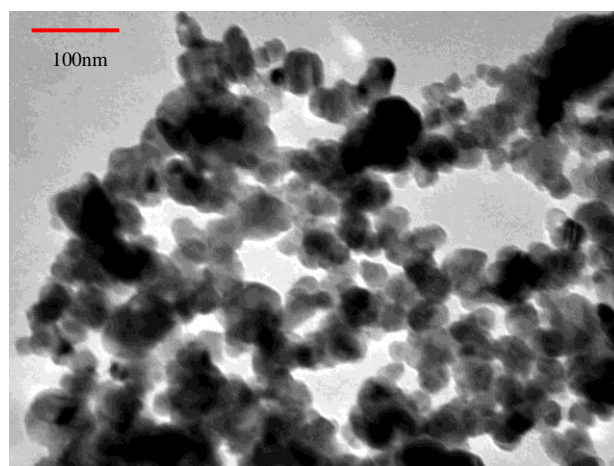
Figure 1 shows that the stability of the turbid liquid composed of dispersing agents of different types and SiC nanoparticles decreases, descending from the use of arabic gum, decyltrimethylammonium bromide, cetyl trimethyl ammonium bromide, to sodium dodecyl benzene sulfonate. When arabic gum is used as dispersing agent, the absorbance of SiC particles in turbid liquid within 4.5 h shows almost no change, which indicates that the SiC particles had the highest stability. Figure 2 shows the influence of arabic gum concentration on SiC stability. When the concentration of arabic gum exceeds  $0.3 \text{ g}\cdot\text{L}^{-1}$ , the absorbance change rate of turbid liquid is low ( $<5\%$ ), which indicates that the stability of SiC changes minimally. When the concentration reaches  $0.45 \text{ g}\cdot\text{L}^{-1}$ , SiC exhibits the best stability. However, considering the impacts caused by excessive arabic gum on the coating, the concentration of arabic gum should remain at  $0.3 \text{ g}\cdot\text{L}^{-1}$ .



(a) cetyltrimethylammonium bromide



(b) decyltrimethylammonium bromide



(c) acacia gum

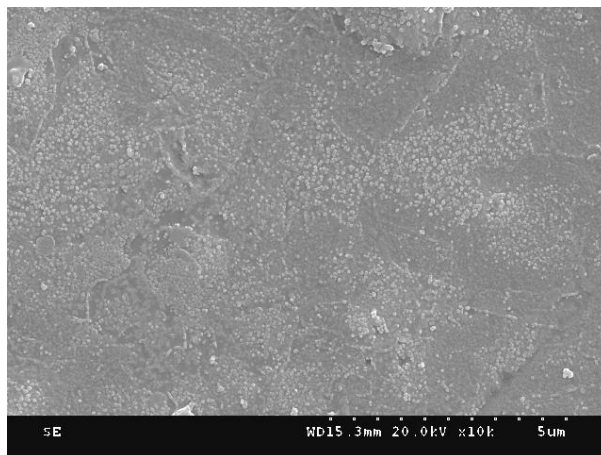
**Figure 3.** TEM image of SiC nanoparticles in different dispersing agent solutions.

Figure 3 shows the TEM image of SiC in different dispersing agents with a concentration of  $0.45 \text{ g} \cdot \text{L}^{-1}$ . When cetyltrimethyl ammonium bromide is used as dispersing agent, SiC has lower dispersibility, with agglomeration occurring while increasing in particle size. On the other hand, decyltrimethylammonium bromide and arabic gum are good for the dispersibility of SiC. When arabic gum is used as dispersing agent (Figure 3c), SiC nanoparticles disperse, and no severe agglomeration occurs with a particle size of about 50 nm. The result corresponds with the test results in Figure 1.

The dispersing mechanism of different surfactants varies in turbid liquid. As ionic surfactants, cetyl trimethyl ammonium bromide, decyltrimethylammonium bromide, and sodium dodecyl benzene sulfonate are adsorbed on the SiC particle surfaces in turbid liquid and changes the zeta electric potential on the surface in which electrostatic repulsion restricts the contact and collision of particles. Arabic gum, being a nonionic surfactant, recognizes the dispersion between particles through steric hindrance due to its large molecular weight and thick adsorption layer. The results of the experiments

above show that steric hindrance conducted by using arabic gum is the main factor in inhibiting agglomeration of SiC particles in turbid liquid.

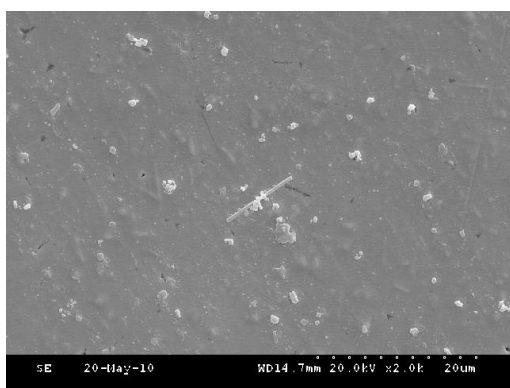
### 3.2 Coating morphology



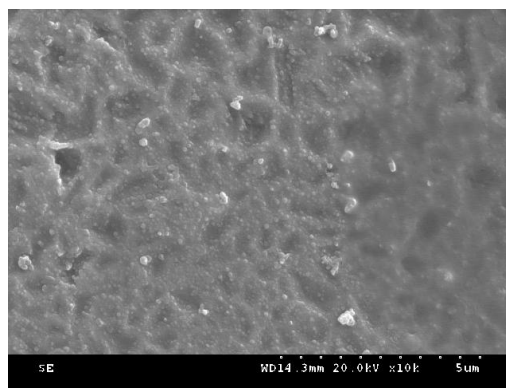
**Figure 4.** SEM image of Sn/SiC nano composite coating.

Under the following conditions,  $\text{Sn}(\text{CH}_3\text{SO}_3)_2$ :  $48.31 \text{ g}\cdot\text{L}^{-1}$ ;  $\text{CH}_3\text{SO}_3\text{H}$  (70%):  $80 \text{ g}\cdot\text{L}^{-1}$ ; hydroquinone:  $2 \text{ g}\cdot\text{L}^{-1}$ ; nanometer SiC (40 nm):  $6 \text{ g}\cdot\text{L}^{-1}$ ; dispersing agent:  $0.3 \text{ g}\cdot\text{L}^{-1}$ ; stirring rate: 200 rpm; brightening agent:  $1 \text{ ml}\cdot\text{L}^{-1}$ ; electric current density:  $3 \text{ A}\cdot\text{dm}^{-2}$ ; temperature:  $25 \text{ }^\circ\text{C}$ , the SEM image shown in Figure 4 shows coating surface evenness, refined matrix metallic Sn crystallization, and evenly distributed SiC.

During the experiment, the concentration of nanoparticles in the plating bath has great impact on the coating morphology. To investigate the influence of SiC concentration on the microcosmic morphology of coating, SiC nanoparticles changed under electrodeposition, and their concentration was also altered in the plating bath.



(a)



(A)

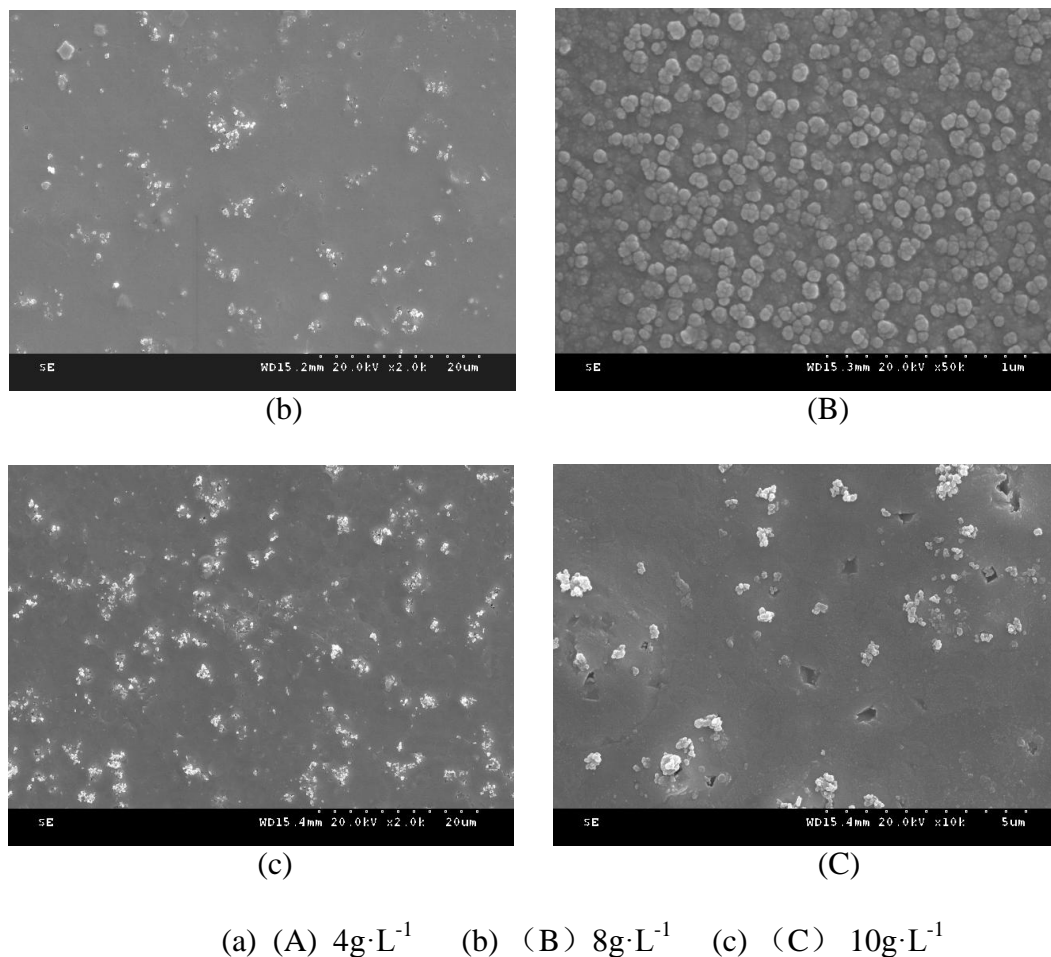


**Figure 5.** Influences of SiC concentration on the microcosmic morphology of composite coating.

In Figure 5, the influence of SiC nanoparticles on coating morphology are shown, with two SEM images of different amplification factors of the coating obtained under the same condition. When the concentration of SiC nanoparticles in the plating bath changed within the range of  $4\text{ g}\cdot\text{L}^{-1}$  to  $10\text{ g}\cdot\text{L}^{-1}$ , the coating morphology showed obvious changes. When the concentration of SiC particles is lower than  $8\text{ g}\cdot\text{L}^{-1}$ , the obtained coating becomes smoother and more even, and its crystal grains became more refined. At the same time, SiC particles are distributed more evenly and no severe agglomeration was observed. The deposited matrix metallic Sn crystallization reaches nanoscale with SiC concentration of  $8\text{ g}\cdot\text{L}^{-1}$  (Figure 5b). However, when SiC concentration exceeds  $8\text{ g}\cdot\text{L}^{-1}$ , the matrix Sn crystal particles were thick and unevenly coated. Figure 5c shows agglomeration in the nanoparticles and holes in the coating surface. Therefore, coating with even and refined crystal particles can be obtained when the SiC concentration remains at  $8\text{ g}\cdot\text{L}^{-1}$ . The addition of nanoparticles can improve the cathodic polarization curve of electrodeposition, as shown in Figure 6. With the increase of SiC particle concentration in the plating bath, a negative potential shift was observed in the cathode, and the degree of cathodic polarization increased. In addition, the ionic dispersion was

restricted, and ohmic polarization of the solution increased. At the same time, the real surface area on the cathode decreased while the electric current density increased when the particles entered the coating, and the cathode precipitated to further increase the degree of cathodic polarization. As more SiC particles are added into the plating bath, the action is more obvious and overpotential increases. Therefore, SiC nanoparticles in the plating bath will change the overpotential to achieve metal nucleation and a new crystal nucleus growing point. This will provide more growing centers for the electrode interface during electrodeposition and effectively restrain crystal growth. Therefore, the refining effects of SiC nanoparticles on matrix metal crystal grains are remarkable.

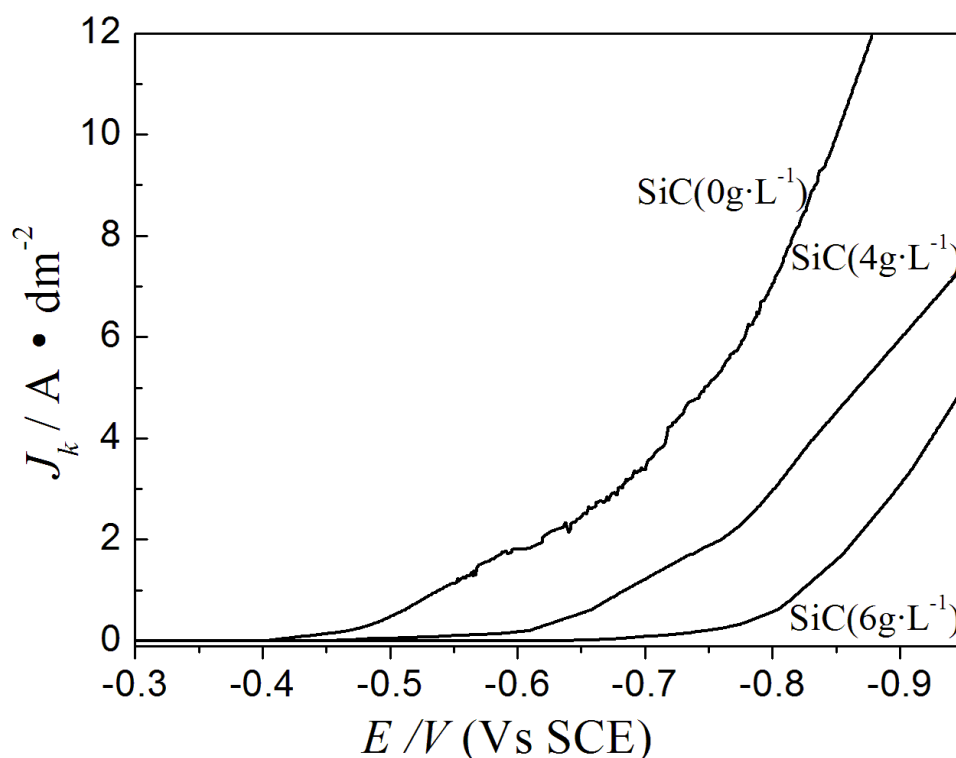


**Figure 6.** Influences of SiC concentration on cathodic polarization curve.

In the coating, the smaller the grains are, the more the grains are, and more grains will increase grain boundaries between grains and between nano SiC and grains, which are areas where many dislocations occur. These changes are advantageous to the absorption and relaxation of inner stress in grain boundaries. As a result, the ability to restrict the growth of Sn whiskers of this coating is superior to that of tin and tin alloy coating.

However, high SiC concentration increases the possibility of agglomeration and sedimentation because of collision between particles, which increases the difficulty of adsorption and deposition in the cathode. Falling particles will affect the morphology of the coating. Furthermore, numerous changes in the cathode area will increase the electric current density excessively, which will scorch the coating.

3.3 Constitution of the coating

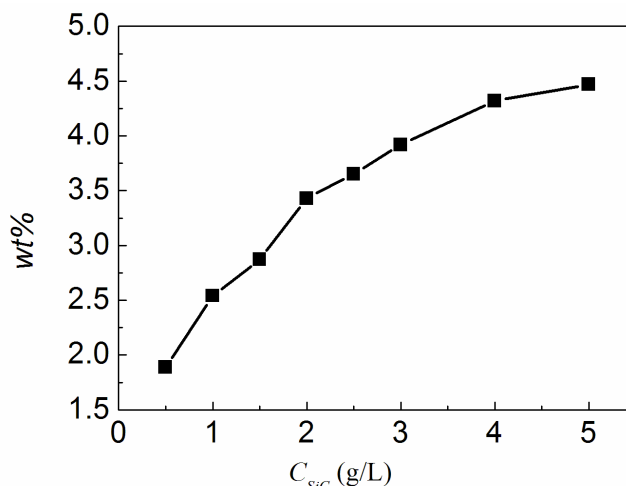


**Figure 7.** Influences of SiC concentration on SiC content in the coating.

Figure 7 shows the influences of SiC concentration in the coating when its concentration in the plating bath remains between  $0.5 \text{ g}\cdot\text{L}^{-1}$  to  $5 \text{ g}\cdot\text{L}^{-1}$ . SiC content in the coating increases along with the increase of SiC concentration in the plating bath, with the highest point reaching 4.47%. However, when SiC concentration exceeds  $4 \text{ g}\cdot\text{L}^{-1}$ , SiC content in coating changed minimally. Also, excessive SiC concentration will lead to a coarse coating surface and bad morphology.

The composite co-electrodeposition between SiC nanoparticles in a methanesulfonic acid system and Sn conforms to the Guglielmi two-step adsorption mechanism, which suggests that the strong and weak adsorptions between SiC particles and cathode play important roles. The relationship between a compound quantity of the particles in coating and particle concentration in plating bath is shown below (1):

$$\frac{C}{\alpha} = \frac{Wi_0}{nF\rho v_0} \cdot e^{A-B} \eta \left( \frac{1}{K} + C \right) \tag{1}$$

where C is the particle concentration in the plating bath,  $\alpha$  is the particle content in the coating, F is the Faraday’s constant, W denotes the atomic weight of precipitated metal,  $\rho$  is the density of precipitated metal,  $i_0$  is the exchange current density[12],  $\eta$  is the precipitated overpotential, n represents the valence state of precipitated ionic, and  $v_0$ , A, and B are constants.

When SiC concentration is low in the plating bath, particles do not affect the electric conductivity of the plating bath, and deposition quantity of particles is only related to SiC concentration in the plating bath. At the same time, with increased SiC concentration, nanoparticles are transferred into the cathode. The increased quantity of collision and adsorption on the cathode surface increases the odds for SiC to be covered and coated by the deposited metallic Sn, which increases the

deposition quantity. However, along with the excessive concentration of solid particles in plating bath, the odds increased for collisions between particles and then subsided due to agglomeration. This affects the SiC content in the coating. At the same time, the electrical conductivity of the plating bath is lessened because of the presence of excessive non-conductive particles. Therefore, the  $i_0$  in Formula (1) decreases and  $\frac{C}{\alpha} - C$  cannot be used. At this time, weak adsorption keeps increasing, finally leading to the reduction of deposition quantity.

### 3.4 Structure of the coating

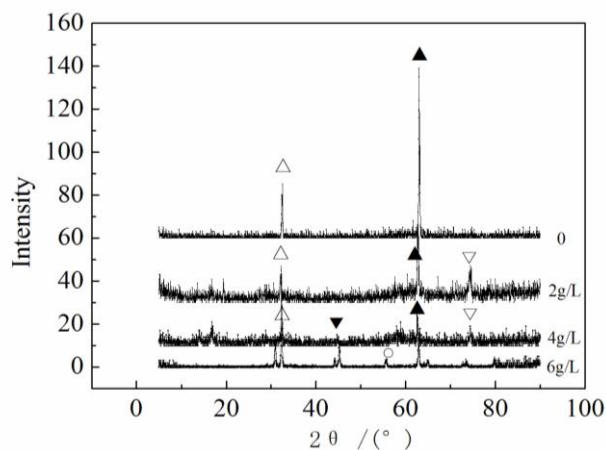


**Figure 8.** Influences of SiC concentration on the XRD images of Sn/SiC composite coatings.

SiC nanoparticle concentration in the plating bath changes not only the constitution and appearance of the coating, but also affects the growth orientation and coating properties of the metallic Sn crystal plane. The XRD image in Figure 8 shows the influences of SiC dosage on the coating.

The test was conducted under the following conditions: Cu target: ( $K\alpha$ ,  $\lambda = 0.15406$  nm); X-ray tube voltage: 40 kV; current: 30 mA; scanned area:  $5^\circ$  to  $90^\circ$ , and; scanning rate:  $6^\circ \cdot \text{min}^{-1}$ .

Figure 8 shows that different SiC particle concentrations will lead to different crystal intensity indices of grains in the coating. This condition indicates that the addition of SiC influences the orientation growth of Sn on different crystal planes. The preferred orientation growth of (101) crystal plane and (112) crystal plane is manifested on the pure Sn coating with no SiC, where crystal plane (112) has the strongest diffraction peak. The preferred growth of crystal plane of pure Sn coating grains changes along with increased SiC particle concentrations (when SiC concentration reaches  $2 \text{ g} \cdot \text{L}^{-1}$ ). Diffraction peaks of crystal planes (101), (112), and (420) of Sn appear when  $2\theta$  reaches  $32.3^\circ$ ,  $62.8^\circ$ , and  $73.2^\circ$ , respectively. Crystal plane (112) has the strongest diffraction peak, and the relative intensity of the diffraction peaks of crystal planes (112) and (101) exhibits almost no changes. When the SiC nanoparticle concentration increases to  $4 \text{ g/L}$ , the relative intensity of the diffraction

peak of crystal plane (101) increases compared with that of (112), whereas no considerable change in the intensity was observed on plane (420). This indicates that the preferred orientation of crystal plane (112) is restricted during the growth process of crystal planes. When the SiC concentration reaches 6 g/L, the orientation of crystallization changes significantly. The strongest diffraction peak was observed on crystal plane (101), followed by crystal plane (112), whereas no diffraction peak was observed on crystal plane (420). However, a diffraction peak is present on (221), which indicates that the original (112) crystal plane grew and transferred to crystal plane (101). However, because of excessive SiC in the plating bath and when  $2\theta=57.5$ , the deposition rate of Sn slows and the coating surface is coarse, which leads to partial thinness and the occurrence of a copper matrix. This condition is probably due to low SiC content, so no obvious SiC diffraction peak appears in the diffraction patterns.

Figure 8 shows that the diffraction peak width of crystal plane (112) increased in the coating with SiC nanoparticles compared with the pure Sn coating. This condition indicates that the addition of SiC will refine coating grains[13].

### 3.5 Performance of coating

#### 3.5.1 Corrosion resistance

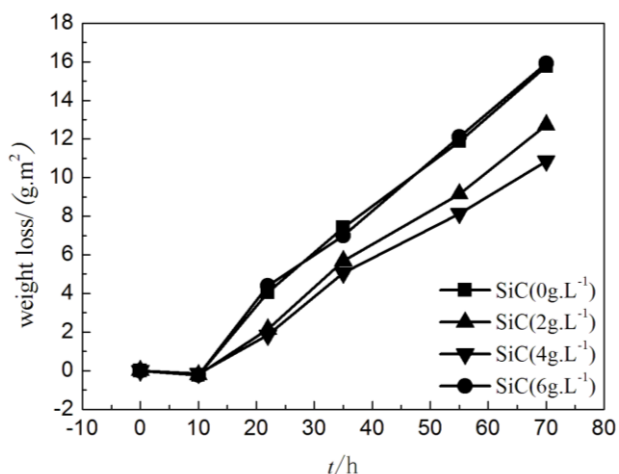


**Figure 9.** Investigation of corrosion resistance of Sn/SiC nano composite coating.

Five percent NaCl mass aqueous solution is prepared with pH adjusted to 3.5 by acetic acid. Pure Sn coating and Sn-SiC nano composite coating was dipped into the solution in the plating bath to investigate the influence of SiC concentration on the corrosion resistance of the coating. The results of the corrosion weight loss coating are shown in Figure 9. During the initial phase within 10 h, the coating quality increases somewhat when coatings are dipped in the corrosive liquid, which may generate insoluble corrosion products like  $\text{Sn}(\text{OH})_2$ ,  $\text{SnO}_2$ , and  $\text{SnO}$ . However, along with increased

corrosion time, products are constantly corroded and dissolved, which decrease coating quality. A comparison between the weight loss of the different coatings showed that the weight loss of composite coating which contains SiC nanoparticles is lower than that of pure Sn coating. When SiC concentration is lowered from  $4 \text{ g}\cdot\text{L}^{-1}$ , the weight loss is reduced along with increased SiC concentration in the plating bath. However, when the concentration reaches  $6 \text{ g}\cdot\text{L}^{-1}$ , the corrosion weight loss of the coating increased significantly. This result indicates that the presence of an appropriate amount of SiC nanoparticles in the coating may improve the corrosion resistance of Sn coating because of the grain refinement caused by the addition of SiC as well as the chemical inertness of SiC. On the other hand, excessive SiC particle concentration will not only result in coarse Sn grains but also reduce the content of SiC particles in the coating because of the agglomeration of SiC nanoparticles. This condition produces holes on the surface and does not improve corrosion resistance, which is the same as what was researched in some journals. A. Vlasa et al[14]. also made researches on corrosion resistance of Zn-TiO<sub>2</sub> nanocomposite coatings, which indicated that dispersed nano particles in coating made grains refined. Smooth and compact coating can decrease porosity and improve corrosion resistance.

### 3.5.2 Electrochemical test

The influence of SiC concentration in the plating bath on corrosion current and corrosion potential of the coating are investigated by using the electrochemical test system to test the Tafel curve of composite coating in 2.5% (mass) NaCl solution; the results are shown in Figure 10 and Table 1. When SiC concentration in the plating bath is increased from 0 to  $4 \text{ g}\cdot\text{L}^{-1}$ , the corrosion potential of Sn/SiC nanocomposite coating gradually became negative, and corrosion current reduced. When the concentration reaches  $4 \text{ g}\cdot\text{L}^{-1}$ , the corrosion current density reached the lowest value of  $4.76 \times 10^{-6} \text{ A}\cdot\text{cm}^{-2}$  which indicates the strongest corrosion resistance of the coating. Meanwhile, the corrosion current density of composite coating is close to that of Sn-Ag-Cu[15] and Sn-Pb[16] alloy coating researched in some journals. The value is the same order of magnitude, indicating the corrosion resistance of nanocomposite coating is as the same as that of Sn-Ag-Cu and Sn-Pb alloy coating. The results of this test correspond with that of corrosion weight loss.

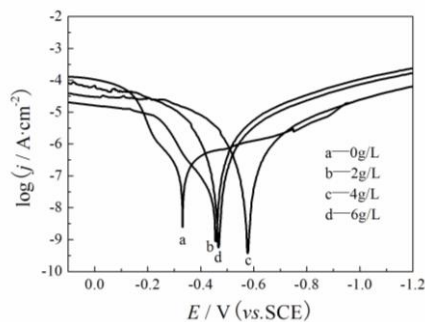


**Figure 10.** Tafel curve of Sn/SiC nanocomposite coating in 3.5% NaCl solution.

**Table 1.** Test results of Sn/SiC nano composite coating corrosion current and corrosion potential.

SiC concentration $C$ ( $\text{g}\cdot\text{L}^{-1}$ )	Corrosion Current Density $j_{\text{corr}}$ ( $10^{-6} \text{A}\cdot\text{cm}^{-2}$ )	Corrosion Potential $E(\text{V})$
0	5.78	-0.34
2	5.13	-0.39
4	4.76	-0.44
6	4.92	-0.41

#### 4. CONCLUSION

This paper put forward new technology to strengthen and improve pure tin coating by adding SiC particle into the it. Sn/SiC nanoparticle composite coating was prepared through electrodeposition in a methanesulfonic acid system, and the influencing rules of SiC concentration on coating morphology, structure, and corrosion resistance performance were obtained.

1. Arabic gum is good for the dispersion and stability of SiC nanoparticles. SiC nanoparticles can form a stable dispersed system in  $0.3 \text{ g}\cdot\text{L}^{-1}$  arabic gum aqueous solution.

2. Adding an appropriate amount of SiC nanoparticles to coating can produce evenness and grain refinement. SiC content in the coating increases along with the increase of SiC concentration in the plating bath. Under the experiment conditions mentioned in the paper, SiC content in alloy coating does not change significantly when SiC concentration exceeds  $4 \text{ g}\cdot\text{L}^{-1}$ .

3. The addition of SiC in the plating bath increases the cathodic polarization and refines grains. It also changes the growth orientation of metallic Sn crystallization in the coating, which provides the possibility for suppressing the growth of Sn whisker. The corrosion resistance of the alloy coating is related to the morphology and SiC content. As the grains become more refined, the SiC content in the composite coating increases, and corrosion resistance improves. Moreover, coating with the lowest corrosion current is produced when SiC concentration reaches  $4 \text{ g}\cdot\text{L}^{-1}$  and corrosion resistance is as the same as Sn-Ag-Cu, Sn-Pb alloy coating.

#### ACKNOWLEDGEMENTS

This work was financially supported by the Heilongjiang Provincial Education Department Foundation (No.12521607), Qiqihar University Young Science Foundation (No. 2010k-M17).

#### References

1. Jinqiu Zhang, Maozhong An, Limin Chang, *Electrochimica Acta.*, 54 (2009) 2883.
2. C. S. Lin, K. C. Huang, *J. Appl. Electrochem.*, 34 (2004) 1013.
3. T.Aruna, V. K. William Grips, K. S. Rajam, *J. Appl. Electrochem.*, 40 (2010) 2161.

4. S. T. Aruna, S. V. Ezhil, G. V. K. William, K. S. Rajam, *J. Appl. Electrochem.*, 41 (2011) 461.
5. Yue-Seon Shin, Young-Ki Ko, Jun-Ki Kim, Sehoon Yoo. *Surf. Rev. Lett.*, 17 (2010) 201.
6. Hao Li, Yizao Wan, Hui Liang, Xiaolei Li, Yuan Huang, Fang He, *Appl. Surf. Sci.*, 256 (2009) 1614.
7. P. Gyftou, M. Stroumbouli, E. A. Pavlatou, K. Asimidis, N. Spyrellis, *T. I. Met. Finish.*, 80 (2000) 88.
8. P. Nowak, R.P. Socha, M. Kaisheva, J. Fransaer, J. P. Celis, Z. Stoinov, *J. Appl. Electrochem.*, 30 (2000) 429.
9. C. Zanella, M. Lekka, P. L. Bonora, *J. Appl. Electrochem.*, 39 (2009) 31.
10. Hong-Kee Lee, Ho-Young Lee, Jun-Mi Jeon, *Met Mater Int.*, 14 (2008) 599.
11. B. P. Singh, J. Jena, L. Besra, S. Bhattacharjee, *J. Nanopart. Res.*, 9 (2007) 797.
12. N. N. Phong, N. T. A. Tuyet, D. C. Linh, N. V. Hue, *Met. Mater. Int.*, 12 (2006) 493.
13. A. Dimitrovskal, R. Kovacevic, *J. Electron. Mater.*, 38 (2009) 2516.
14. A. Vlasa , S.Varvara , A.Pop , C.Bulea, L.M. Muresan, *J. Appl. Electrochem.*, 40 (2010) 1519.
15. J. Q. Zhang, Electroplating Process and Mechanism of Tin-Silver-Copper Alloy and Solder of Deposits, Dissertation for the Doctoral Degree in Engineering, Harbin Institute of Technology, Harbin(2009).
16. Z.X.Hu, X.H.Jie, G.H.Lu. Corrosion resistance of Pb–Sn composite coatings reinforced by carbon nanotubes. *J. Coat. Technol. Res.*, 7 (2010) 809.